


## Fixed Depth Hamiltonian Simulation via Cartan Decomposition

Efekan Kökcü<sup>1,\*</sup>, Thomas Steckmann<sup>1</sup>, Yan Wang<sup>2</sup>, J. K. Freericks<sup>3</sup>,  
Eugene F. Dumitrescu<sup>2,†</sup> and Alexander F. Kemper<sup>1,‡</sup>

<sup>1</sup>*Department of Physics, North Carolina State University, Raleigh, North Carolina 27695, USA*

<sup>2</sup>*Oak Ridge National Laboratory, Computational Sciences and Engineering Division, Oak Ridge, Tennessee 37831, USA*

<sup>3</sup>*Department of Physics, Georgetown University, 37th and O Streets NW, Washington, D.C. 20057, USA*

 (Received 3 May 2021; revised 9 April 2022; accepted 28 June 2022; published 9 August 2022)

Simulating quantum dynamics on classical computers is challenging for large systems due to the significant memory requirements. Simulation on quantum computers is a promising alternative, but fully optimizing quantum circuits to minimize limited quantum resources remains an open problem. We tackle this problem by presenting a constructive algorithm, based on Cartan decomposition of the Lie algebra generated by the Hamiltonian, which generates quantum circuits with time-independent depth. We highlight our algorithm for special classes of models, including Anderson localization in one-dimensional transverse field  $XY$  model, where  $\mathcal{O}(n^2)$ -gate circuits naturally emerge. Compared to product formulas with significantly larger gate counts, our algorithm drastically improves simulation precision. In addition to providing exact circuits for a broad set of spin and fermionic models, our algorithm provides broad analytic and numerical insight into optimal Hamiltonian simulations.

DOI: 10.1103/PhysRevLett.129.070501

Constructing arbitrary unitary operations as a sequence of 1- and 2-qubit gates is the task of “unitary synthesis,” which has applications from quantum state preparation (e.g., via the unitary coupled cluster formalism [1,2]) to quantum arithmetic logic. A paradigmatic problem [3,4] is the unitary synthesis of time evolution under a time-independent Hamiltonian  $\mathcal{H}$ . Hamiltonian evolution plays a key role in simulating quantum systems on quantum computers [5–9] and thus has spurred recent interest in order to solve difficult problems beyond the scope of classical computing. It involves solving  $i(d/dt)|\psi(t)\rangle = \mathcal{H}|\psi(t)\rangle$  via the unitary  $U(t) = e^{-i\mathcal{H}t}$ , which yields  $|\psi(t)\rangle = U(t)|\psi(t=0)\rangle$ . While the circuit complexity for an arbitrary unitary grows exponentially with the number of qubits, there are efficient product formulas [6,10,11], series expansions [12], and other techniques [13–15] for Hamiltonian simulation.

Despite these algorithms’ efficient asymptotic performance, the fast fidelity decay with respect to circuit depth before error correction prevents useful Hamiltonian simulation in near term hardware [16]. Reducing the circuit depth required for simulations remains of interest and recent works have begun to incorporate additional problem information such as algebraic properties, system symmetries [17], and initial state properties [18] to further improve Hamiltonian time evolution. Orthogonally, variational approaches have been used to approximate the time evolution [19], but the approximation worsens with increasing time.

Concurrent with the above synthesis techniques, Cartan decomposition emerged as a useful tool in the areas of

quantum control [20,21] and time evolution [22]. An optimal unitary synthesis of arbitrary 2-qubit operations based on the Cartan decomposition has emerged as the state-of-the-art technique [23]. For larger unitaries, Refs. [24–27] have formally laid out how any element in  $SU(2^n)$  can be decomposed, although these methods generally require exponential circuit depth for *arbitrary* unitaries and recursive algorithms [24,26,27]. The product factorization works as follows: consider a generic time-independent Hamiltonian for  $n$  qubits (or  $n$  spin- $1/2$  particles)

$$\mathcal{H} = \sum_j H_j \sigma^j, \quad (1)$$

where  $H_j$  are real coefficients and  $\sigma^j$  are Pauli string operators: i.e., elements of the  $n$ -site Pauli group  $\mathcal{P}_n = \{I, X, Y, Z\}^{\otimes n}$ . Reference [24] recursively obtains a factorization of the time-evolution unitary as

$$U(t) = e^{-i\mathcal{H}t} = \prod_{\vec{\sigma}^i \in \mathfrak{su}(2^n)} e^{i\kappa_i \vec{\sigma}^i}, \quad (2)$$

with, in the general case,  $\mathcal{O}(4^n)$  angles  $\kappa_i$  for the Pauli strings  $\vec{\sigma}^i$  that form a basis for the Lie algebra  $\mathfrak{su}(2^n)$ .

We now provide a constructive decomposition algorithm for Hamiltonian simulation with depth independent of simulation time. We begin by applying Cartan decomposition on a subalgebra of  $\mathfrak{su}(2^n)$  generated from the Hamiltonian. We further simplify the subsequent problem of finding the parameters  $\kappa_i$  to locating a *local* extremum,

rather than global minimum, of a cost function by extending the method given in Refs. [28,29]. This extension allows us to directly generate a circuit and calculate the cost function and its gradient. The algorithm is applicable to *any* model without limitations of locality, although the scaling varies depending on the model, and we provide software to do so [30].

For certain classes of models (termed “fast-forwardable” [31]), such as spin models that can be mapped to noninteracting fermion models [32], the circuit complexity and calculation of the cost function scales polynomially in the system size. To illustrate our algorithm, we use it to time evolve a ten-site random transverse field XY (TFXY) model and compare the result to a Trotter approach to illustrate the dramatic improvements obtained.

*Hamiltonian algebra.*—For a given Hamiltonian, we determine whether the entirety of  $\mathfrak{su}(2^n)$  is necessary for the expansion in Eq. (2), or whether a subset suffices. The Baker-Campbell-Hausdorff theorem states that only nested commutators of the individual terms in the Hamiltonian appear in the final exponent. This leads us to the first step of our algorithm:

Step 1: Using the expansion of the Hamiltonian in terms of the Pauli terms  $\sigma^j$  in Eq. (1), find the closure (under commutation) of the set of those Pauli terms. This closure forms a basis for the “Hamiltonian algebra,” which we denote as  $\mathfrak{g}(\mathcal{H})$  and which is a subalgebra of  $\mathfrak{su}(2^n)$  [21]. We can now restrict the expansion in Eq. (2) to only the elements of  $\mathfrak{g}(\mathcal{H})$ .

We now provide some examples on the scope and limitations of our resource cost across selected spin Hamiltonians. Figure 1 illustrates the dimension of the Hamiltonian algebra  $|\mathfrak{g}(\mathcal{H})|$  for various models of interest as a function of system size  $n$ , where  $|\cdot|$  denotes the dimension of the algebra. The dimensions of the

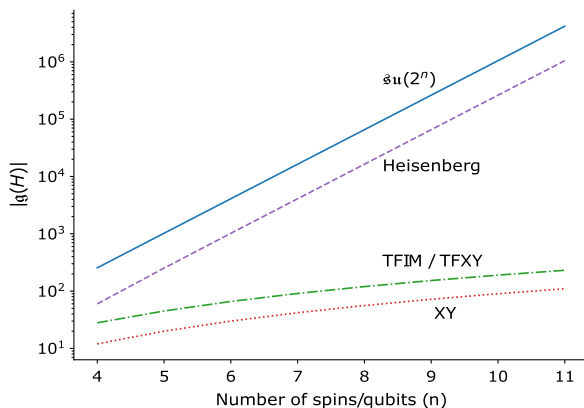


FIG. 1. Hamiltonian algebra dimensions of the nearest-neighbor Heisenberg, XY, TFXY models, and TFIM and dimension of full  $\mathfrak{su}(2^n)$  for comparison to the generic case. The dimensions can exactly be calculated as  $|\mathfrak{g}(\text{Heisenberg})| = 4^{n-1} - 4$ ,  $|\mathfrak{g}(\text{TFIM})| = |\mathfrak{g}(\text{TFXY})| = n(2n - 1)$ , and  $|\mathfrak{g}(\text{XY})| = n(n - 1)$ .

Hamiltonian algebra for the  $n$ -site nearest-neighbor XY, transverse field Ising model (TFIM), and TFXY model are  $|\mathfrak{g}(\text{XY})| = n(n - 1)$  and  $|\mathfrak{g}(\text{TFIM})| = |\mathfrak{g}(\text{TFXY})| = n(2n - 1)$ ; these scale *quadratically* with the number of qubits  $n$ . On the other hand,  $|\mathfrak{g}(\mathcal{H})|$  for the nearest-neighbor Heisenberg model scales exponentially,  $|\mathfrak{g}(\text{Heisenberg})| = 4^{n-1} - 4$ . We observe a similar exponential growth in the TFXY model and TFIM with longer range interactions. However, even in these cases,  $|\mathfrak{g}(\mathcal{H})|$  is a constant factor smaller than  $|\mathfrak{su}(2^n)|$ , providing a commensurate improvement in circuit depth over the generic case studied in Ref. [24].

*Cartan decomposition.*—We must now determine the parameters  $\kappa_i$  in the  $\mathfrak{g}(\mathcal{H})$  restriction of Eq. (2). The Cartan decomposition and related methods in Refs. [24,28,29] provide the necessary tools to do so. We briefly review the Cartan decomposition and the “*KHK* theorem.”

*Definition 1.*—A Cartan decomposition of a Lie algebra  $\mathfrak{g}$  is defined as an orthogonal split  $\mathfrak{g} = \mathfrak{k} \oplus \mathfrak{m}$  satisfying

$$[\mathfrak{k}, \mathfrak{k}] \subset \mathfrak{k}, \quad [\mathfrak{m}, \mathfrak{m}] \subset \mathfrak{k}, \quad [\mathfrak{k}, \mathfrak{m}] = \mathfrak{m}, \quad (3)$$

and denoted by  $(\mathfrak{g}, \mathfrak{k})$ . A Cartan subalgebra denoted by  $\mathfrak{h}$  refers to a maximal Abelian algebra within  $\mathfrak{m}$ .

We will replace  $\mathfrak{g}$  in Definition 1 above with  $\mathfrak{g}(\mathcal{H}) \subseteq \mathfrak{su}(2^n)$  for a given  $n$ -spin Hamiltonian.

In practice, finding a Cartan decomposition by directly using Definition 1 and picking basis elements one by one is difficult. Instead, the Lie subalgebra is partitioned into  $\mathfrak{k}$  and  $\mathfrak{m}$  by an involution: i.e., a Lie algebra homomorphism taking  $\theta: \mathfrak{g} \rightarrow \mathfrak{g}$ , which satisfies  $\theta[\theta(g)] = g$  for any  $g \in \mathfrak{g}$  and preserves all commutators. Then by using the involution, one can split the algebra by defining subspaces via  $\theta(\mathfrak{k}) = \mathfrak{k}$  and  $\theta(\mathfrak{m}) = -\mathfrak{m}$ , which is equivalent to Definition 1. We discuss further details of involutions in the Supplemental Material [33].

A consequence of Cartan decomposition, which we will use to synthesize Hamiltonian evolution unitaries, is an extension of the *KHK* theorem:

*Theorem 1.*—Given a Cartan decomposition  $\mathfrak{g} = \mathfrak{k} \oplus \mathfrak{m}$  and a nondegenerate invariant bilinear form  $\langle \cdot, \cdot \rangle$  on  $\mathfrak{g}$ , then for any  $m \in \mathfrak{m}$  there exists a  $K \in e^{i\mathfrak{k}}$  and an  $h \in \mathfrak{h}$ , such that

$$m = KhK^\dagger, \quad (4)$$

where we have generalized the *KHK* theorem to any Lie algebra that has a nondegenerate invariant bilinear form. This statement is proven by construction via Theorem 2 (see Supplemental Material [33]). We use  $\langle A, B \rangle = \text{tr}(AB)$ , which is proportional to the Killing form in  $\mathfrak{su}(2^n) \supset \mathfrak{g}(\mathcal{H})$  and is therefore guaranteed to be nondegenerate due to semisimplicity of  $\mathfrak{su}(2^n)$ . Moreover, it is invariant and symmetric due to the cyclic property of the trace.

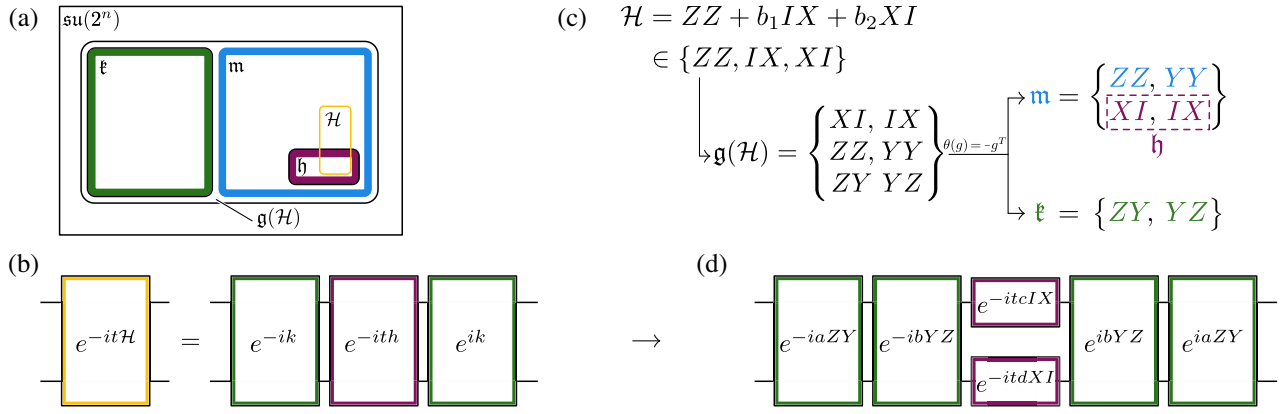


FIG. 2. (a) Schematic relationship of the Hamiltonian algebra  $\mathfrak{g}(\mathcal{H})$  and its partitioning into a subalgebra  $\mathfrak{k}$ , its complement  $\mathfrak{m}$ , and the Cartan subalgebra  $\mathfrak{h}$ . (b)  $KHK$  decomposition (Theorem 1) applied to a time-evolution operator generated by an element of  $\mathfrak{m}$ . (c) Hamiltonian algebra  $\mathfrak{g}(\mathcal{H})$  for the two-site TFIM and the Cartan decomposition generated by the involution  $\theta(\mathfrak{g}) = -\mathfrak{g}^T$ . Here we list the bases that span  $\mathfrak{g}(\mathcal{H})$  and its Cartan decomposition. (d) Decomposed time evolution for the two-site TFIM.

We can now describe the second step of our algorithm:

Step 2: Find a Cartan decomposition of  $\mathfrak{g}(\mathcal{H})$  such that  $\mathcal{H} \in \mathfrak{m}$  (in practice, one finds an involution) and find a Cartan subalgebra  $\mathfrak{h} \subseteq \mathfrak{m}$ . A direct application of Theorem 1 with  $\mathcal{H} = KhK^\dagger$  then leads to the desired unitary for time evolution

$$U(t) = e^{-i\mathcal{H}t} = Ke^{-ith}K^\dagger. \quad (5)$$

Since  $\mathfrak{h}$  is Abelian, each Pauli string in  $h \in \mathfrak{h}$  commutes, and therefore a quantum circuit for  $e^{-ith}$  can easily be constructed. This reduces the circuit construction problem to finding  $K$ , which we address below.

As long as an involution is found such that  $\theta(\mathcal{H}) = -\mathcal{H}$ , this method is applicable to any Hamiltonian  $\mathcal{H}$ . Specifically, for the models discussed in Fig. 1, this step is achieved by using the involution  $\theta(\mathfrak{g}) = -\mathfrak{g}^T$ , which is an AI type Cartan decomposition for  $\mathfrak{su}(2^n)$ . This involution works because the listed models have time reversal symmetry [25]. We then construct  $\mathfrak{h}$  by choosing an element of  $\mathfrak{m}$  randomly (or with certain symmetries if desired) and finding all the elements in  $\mathfrak{m}$  that are mutually commutative with the chosen element and each other. We discuss further details of finding involutions and Cartan subalgebras in the Supplemental Material [33].

Note that the simulation time  $t$  in Eq. (5) enters as an independent parameter and does not alter the structure of  $K$  or  $h$ . This means that new parameters do not need to be found for different simulation times (although this situation may change for time-dependent Hamiltonians).

*Determining parameters.*—We provide the following theorem to determine the group element  $K$  in Eq. (5), which is an improved version of Lemma 6.3 (iii) in [28] and Eq. (18) in [29]:

*Theorem 2.*—Assume a set of coordinates  $\vec{\theta}$  in a chart of the Lie group  $e^{i\mathfrak{k}}$ . For  $\mathcal{H} \in \mathfrak{m}$ , define the function  $f$

$$f(\vec{\theta}) = \langle K(\vec{\theta})vK(\vec{\theta})^\dagger, \mathcal{H} \rangle, \quad (6)$$

where  $\langle \dots \rangle$  denotes a nondegenerate invariant bilinear form on  $\mathfrak{g}$ , and  $v \in \mathfrak{h}$  is an element whose exponential map is dense in  $e^{i\mathfrak{h}}$ . Then for any local extremum of  $f(\vec{\theta})$  denoted by  $\vec{\theta}_c$ , and defining the critical group element  $K_c = K(\vec{\theta}_c)$ , we have

$$K(\vec{\theta}_c)^\dagger \mathcal{H} K(\vec{\theta}_c) = K_c^\dagger \mathcal{H} K_c \in \mathfrak{h}. \quad (7)$$

According to the theorem, we only need to find a local extremum of  $f(\vec{\theta})$ , without determining the resulting  $h \in \mathfrak{h}$ . This is achieved by using  $v$  such that  $e^{iv}$  is dense in  $e^{i\mathfrak{h}}$ ; this is sufficient to represent the entirety of  $\mathfrak{h}$ . This reduces the number parameters from  $|\mathfrak{k}| + |\mathfrak{h}|$  to  $|\mathfrak{k}|$ . Since we consider single Pauli strings as basis elements, we can choose  $v = \sum_i \gamma_i h_i$ , where the  $h_i$  are basis elements of  $\mathfrak{h}$ , and the  $\gamma_i$  are mutually irrational [29]. After determining  $K_c$ , the  $h \in \mathfrak{h}$  in Eq. (5) is then obtained via Eq. (7). Further details and the proof of the theorem are discussed in the Supplemental Material [33].

Because the parametrization does not need to cover the entire  $e^{i\mathfrak{k}}$ , there is a choice in how to represent the group element  $K$  in Theorem 2. While Refs. [24,29] use  $K = \exp(i \sum_i \alpha_i k_i)$ , we express it as a factorized product

$$K = \prod_i e^{i\alpha_i k_i}, \quad (8)$$

where  $k_i$  is an element of the Pauli string basis for  $\mathfrak{k}$ . The representation (8) does not always cover  $e^{i\mathfrak{k}}$  fully, except in some specific cases [34,35], but this is not necessary [33]. However, using Eq. (8) has three benefits. First, the gradient of Eq. (6) can be obtained analytically at any point, in contrast to the complicated derivative of the exponential map  $\exp(i \sum_i \alpha_i k_i)$ ; second, this allows us

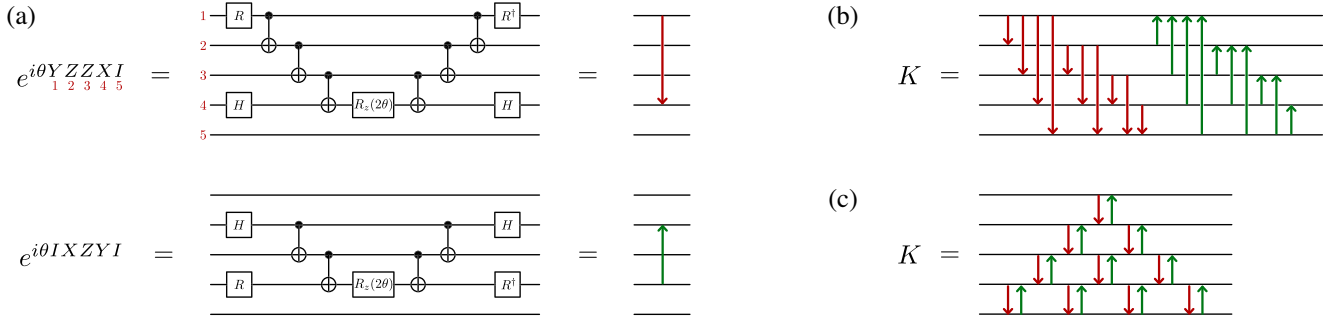


FIG. 3. (a) Circuit implementation of the given exponentials of Pauli strings and the compact arrow notation. The  $R$  gate shown here is  $R_x(\pi/2)$ . (b) Unoptimized and (c) optimized circuit for  $K$  in an  $n = 5$ -site TFXY model (this system size is chosen for illustrative purposes). The circuits have  $\mathcal{O}(n^3)$  (80) and  $\mathcal{O}(n^2)$  (20) controlled NOT (CNOT) gates, respectively.

to apply  $K$  on  $v$  and  $\mathcal{H}$  exactly [33]; and third, since a circuit implementation for exponentiated individual Pauli strings is known [36,37], we avoid the need for further decomposition of  $K$ .

We now reach the third step of our algorithm:

Step 3: Minimize Eq. (6) over the parameters  $a_i$  in  $K$  in Eq. (8) to find  $K \in e^{i\mathfrak{k}}$ . In this Letter, we use a standard Broyden-Fletcher-Goldfarb-Shanno optimization routine. Calculating Eq. (6) and its gradient and obtaining  $h \in \mathfrak{h}$  by using Eq. (8) requires  $\mathcal{O}(|\mathfrak{k}||\mathfrak{m}|)$ ,  $\mathcal{O}(|\mathfrak{k}|^2|\mathfrak{m}|)$ , and  $\mathcal{O}(|\mathfrak{k}||\mathfrak{m}|)$  operations, respectively. For models where  $|\mathfrak{g}(\mathcal{H})|$  is quadratic in the number of spins, these become  $\mathcal{O}(n^4)$ ,  $\mathcal{O}(n^6)$ , and  $\mathcal{O}(n^4)$  [33].

In summary, our algorithm can be listed as the following three steps: 1. Construct the Hamiltonian algebra  $\mathfrak{g}(\mathcal{H})$ . 2. Find a suitable Cartan decomposition (or involution) such that  $\mathcal{H} \in \mathfrak{m}$ , and construct a Cartan subalgebra  $\mathfrak{h}$ . 3. Find a local extremum of  $f(\vec{\theta})$  by representing  $K$  as in Eq. (8), obtain  $h \in \mathfrak{h}$  via Eq. (7), and then construct the circuit.

Figure 2 is a schematic illustration of the algorithm. Figure 2(a) shows the relationships between  $\mathfrak{su}(2^n)$ , the Hamiltonian  $\mathcal{H}$ , the Hamiltonian algebra  $\mathfrak{g}(\mathcal{H})$ , and its Cartan decomposition. Figure 2(b) shows the resulting factorization of the time-evolution operator. Figures 2(c) and 2(d) demonstrate steps 1 and 2 of our algorithm for a simple two-site Ising model. In this case, the Hamiltonian terms  $\{ZZ, IX, XI\}$  generate a six-dimensional Hamiltonian algebra  $\mathfrak{g}(\mathcal{H})$ , which is partitioned into  $\mathfrak{k}$  and  $\mathfrak{m}$  via the involution  $\theta$ . Among infinitely many possibilities, there are two maximal Abelian subalgebras  $\mathfrak{h}$  of  $\mathfrak{m}$  that have single Pauli strings as basis elements (rather than a linear combination of them), namely,  $\text{span}\{ZZ, YY\}$  and  $\text{span}\{XI, IX\}$ ; we choose the latter without loss of generality. The resulting factored time-evolution operator is shown in Fig. 2(d). This factorization is clearly suboptimal for the Hamiltonian evolution unitary in  $\text{SU}(4)$ , where a minimal three-CNOT circuit is known [23]; however, our decomposition algorithm is applicable to any system size.

*Application.*—To demonstrate the flexibility of our method, we simulate a ten-site TFXY spin chain with random magnetic field with open boundary conditions, with the Hamiltonian

$$\mathcal{H} = \sum_{i=1}^{n-1} (X_i X_{i+1} + Y_i Y_{i+1}) + \sum_{i=1}^n b_i Z_i, \quad (9)$$

where  $n = 10$  is the number of qubits and the  $b_i$  coefficients are chosen via a normal distribution with zero mean and  $\sigma^2$  variance; we use standard notation for the Pauli spin matrices. We consider a single spin-flip initial state  $|\psi\rangle = |\downarrow\uparrow\uparrow\uparrow\uparrow\uparrow\uparrow\uparrow\uparrow\rangle$ . In the absence of the random magnetic field, this excitation diffuses throughout the system. By increasing the random magnetic field strength, the excitation is prevented from diffusing by amplitude cancellation due to random phases acquired via probing the random magnetic field, which is called the Anderson localization mechanism [38]. Specifically, in one dimension, it was shown that any  $p$ th moment of the displacement of the excitation has a time-independent upper bound [39]  $\langle |\hat{N}|^p \rangle_t < C$ , where  $C$  is a time-independent constant, and the position operator for the excitation is  $\hat{N} = \sum_{r=1}^n (r-1)(1-Z_r/2)$ .

We first perform steps 1 and 2 of our algorithm. The Cartan decomposition and subalgebra for this model are

$$\begin{aligned} \mathfrak{k} &= \text{span}\{\widehat{X}_i \widehat{Y}_j, \widehat{Y}_i \widehat{X}_j | i, j = 1, 2, \dots, n, i < j\}, \\ \mathfrak{m} &= \text{span}\{Z_j, \widehat{X}_i \widehat{X}_j, \widehat{Y}_i \widehat{Y}_j | i, j = 1, 2, \dots, n, i < j\}, \\ \mathfrak{h} &= \text{span}\{Z_i | i = 1, 2, \dots, n\}, \end{aligned} \quad (10)$$

with dimensions  $|\mathfrak{k}| = n(n-1)$ ,  $|\mathfrak{m}| = n^2$ , and  $|\mathfrak{h}| = n$ , and

$$\widehat{A}_i \widehat{B}_j = A_i Z_{i+1} Z_{i+2} \dots Z_{j-1} B_j. \quad (11)$$

We then perform step 3 of our algorithm and find the parameters minimizing Eq. (6).

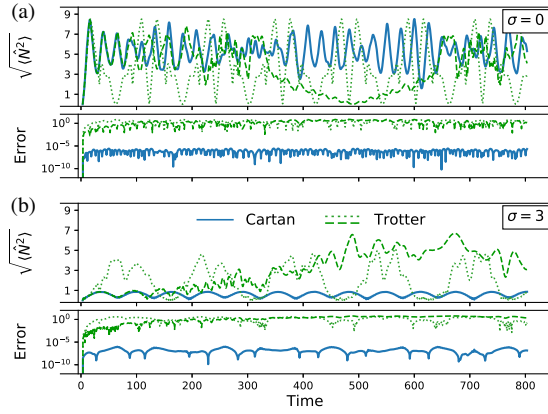


FIG. 4. Displacement of the spin excitation  $N = \sqrt{\langle \hat{N}^2 \rangle}$  and its absolute difference from the exact result  $|N - N_{\text{exact}}|$  in the TFXY model with a random  $Z$  field, for standard deviation  $\sigma = 0$  in (a) and  $\sigma = 3$  in (b). The excitation becomes trapped around its original position as  $\sigma$  increases. The localization is captured to within a small constant error by our Cartan algorithm (solid curves). The two Trotter decompositions use 180 (dotted) and 1332 (dashed) CNOTs, which correspond to the CNOT counts of the optimized and nonoptimized Cartan circuits, respectively.

Using Eq. (8) generates the circuit shown in Fig. 3(b), which has  $2n(n^2 - 1)/3$  CNOT gates (1320 CNOTs for  $n = 10$ ). As illustrated in Fig. 3(c), this circuit can be further simplified to a circuit with  $n(n - 1)$  CNOT gates (180 CNOTs for  $n = 10$ ) (see Supplemental Material [33]). We compare the simulation results conducted via our algorithm to Trotter evolutions with varying time steps and fixed depth (fixed number of CNOTs) that is equal to the optimized (10 steps/180 CNOTs) and the unoptimized Cartan circuits (74 steps/1332 CNOTs).

Figure 4 shows  $N = \sqrt{\langle \hat{N}^2 \rangle}$ , the rms position of the single-spin excitation for various values of  $\sigma$ , as simulated with our algorithm and with Trotter time evolution. We renormalized the Hamiltonian for each standard deviation of the transverse field; i.e.,  $\mathcal{H} \rightarrow [\mathcal{H}/\sqrt{\text{tr}(\mathcal{H}^2)}]$  to eliminate any norm dependence of the time evolution.

As expected, the Trotter evolution diverges from the exact result after some time  $\tau$ , which occurs later if there are more Trotter steps.  $\tau$  depends on the standard deviation of disorder  $\sigma$  in the magnetic field; the results improve with increasing randomness because this decreases the relative diffusion probability for the excitation to hop to another site. Nevertheless, for any value of  $\sigma$  and any number of steps, the Trotter evolution eventually diverges from the exact result.

On the other hand, the result from the Cartan decomposition is indistinguishable from the exact solution. We show the error (absolute deviation from the exact result) for the two methods in Fig. 4. Except for the earliest times, there are 3–5 orders of magnitude less error for the Cartan decomposition approach compared to the Trotter-based approach. The error of the Cartan-based method stems from

the nonzero gradient tolerance used in the optimization step of the algorithm (which was chosen to be  $10^{-6}$ ) and does not increase with simulation time, which shows the suitability of this constant-depth circuit for long-time simulations. While this particular application is for a free-fermionic model, the minimal error does not follow from this property. Rather, it stems from the precise factorization via Cartan decomposition, which is equally applicable to interacting fermion models. However, a similar tolerance may lead to larger errors simply due to the larger number of terms required for the decomposition [Eq. (8)]. Data for Fig. 4 are provided at [40].

*Discussion and applications.*—We have introduced an algorithm based on the Cartan decomposition for synthesizing Hamiltonian time-evolution unitaries and provided software to do so [30]. In contrast to previous related approaches [24,26,27,29], the current work develops *explicit* digital quantum circuit constructions for  $K$  via an implementable factorized form [Eq. (8) and Fig. 3]. An analytic cost function and its derivatives, straightforward circuit construction, and only needing a single optimization for any time  $t$  are several improvements with respect to previous algorithms. We have discussed illustrative and paradigmatic examples where our algorithm’s complexity grows polynomially, as in the TFIM and TFXY spin model. Here the polynomial complexity follows a mapping from the spin representation to a noninteracting (free-)fermionic representation. In this sense, the Hamiltonian algebra reveals the existence of such a map and is complementary to a recent graph-theoretic approach to identify spin models solvable by fermionization [32]. This idea has already formed the basis for related compression algorithms [41,42]. Our work also provides an intuition to understanding heuristic “variational fast-forwarding” methods [19,43,44]; the scaling of the Hamiltonian algebra indicates an upper bound on the required circuit depth.

In addition to the applications demonstrated here, we expect our algorithm and its components to find broader use in more quantum computing application areas. First, our method can be applied directly to simulating *both* free and interacting theories and directly deployed on quantum computers. Although the algebra does not scale favorably in the latter case, circuits for interacting fermionic problems can be composed via our technique nevertheless. Given that near term devices scale poorly with circuit depth, and consequently, simulation time, employing our algorithm to small systems yields results that we are not aware of other methods achieving [45]. Next, a generalization to the unitary coupled cluster (UCC) formalism [1,2,46] is also straightforward. In order to represent the wave function, the UCC applies excitations on an ansatz wave function. The usual Trotter-based approach to construct circuits to do so does not respect the symmetries inherent in the problem—this is true for UCC excitations [47] as well as Hamiltonian evolution [17]; this issue can be addressed either by adding

additional symmetry-restoring terms [17] or constructing explicit symmetry-preserving circuits [47]. Since the Cartan decomposition is exact, it preserves all of the symmetries without further effort, even though the individual terms may break symmetries. We will detail this application area in a future work. This concept of using Cartan decomposition to generate a subcircuit for symmetrized UCC factors—a portion of a larger problem—could be applied as a generic quantum compilation routine.

Looking forward, we expect that perturbative approaches beginning from either the free or only interacting algebras will enable further progress in the development of Hamiltonian evolution algorithms. Symmetries and other problem structures are naturally expressed in the language of Lie algebras and further developments are required to fully utilize problem structure. Interestingly, preliminary findings indicate that imposing symmetry complicates quantum circuit construction, while it reduces the dimension of the Hamiltonian algebra; this interplay between physical symmetry and algebraic analysis for quantum circuits has been recently investigated within the contexts of quantum control theory [48–51] and symmetry-preserving circuits [47,17] and could be combined with the methods presented here in future work.

The ideation, formal development, code development, and manuscript writing were supported by the Department of Energy, Office of Basic Energy Sciences, Division of Materials Sciences and Engineering under Award No. DE-SC0019469 (E. K., T. S., J. K. F., and A. F. K.). Final revision and editing was supported by the National Science Foundation under Grant No. PHY-1818914 (E. K. and A. F. K.). J. F. K. was also supported by the McDevitt bequest at Georgetown University. E. F. D. acknowledges DOE ASCR funding under the Quantum Computing Application Teams program, FWP No. ERKJ347. T. S. was supported in part by the U.S. Department of Energy, Office of Science, Office of Workforce Development for Teachers and Scientists (WDTS) under the Science Undergraduate Laboratory Internship program. Y. W. acknowledges DOE ASCR funding under the Quantum Application Teams program, FWP No. ERKJ335.

---

\*ekokcu@ncsu.edu

†dumitrescu@ornl.gov

‡akemper@ncsu.edu

- [1] B. Cooper and P. J. Knowles, *J. Chem. Phys.* **133**, 234102 (2010).
- [2] J. Lee, W. J. Huggins, M. Head-Gordon, and K. B. Whaley, *J. Chem. Theory Comput.* **15**, 311 (2019).
- [3] B. Bauer, S. Bravyi, M. Motta, and G. Kin-Lic Chan, *Chem. Rev.* **120**, 12685 (2020).
- [4] L. Bassman, M. Urbanek, M. Metcalf, J. Carter, A. F. Kemper, and W. A. de Jong, *Quantum Sci. Technol.* **6**, 043002 (2021).
- [5] R. P. Feynman, *Int. J. Theor. Phys.* **21**, 467 (1982).
- [6] S. Lloyd, *Science* **273**, 1073 (1996).
- [7] D. S. Abrams and S. Lloyd, *Phys. Rev. Lett.* **79**, 2586 (1997).
- [8] C. Zalka, *Proc. R. Soc. A* **454**, 313 (1998).
- [9] S. P. Jordan, K. S. Lee, and J. Preskill, *Science* **336**, 1130 (2012).
- [10] J. Haah, M. B. Hastings, R. Kothari, and G. H. Low, *SIAM J. Comput.* FOCS18 (2021).
- [11] A. M. Childs, Y. Su, M. C. Tran, N. Wiebe, and S. Zhu, *Phys. Rev. X* **11**, 011020 (2021).
- [12] D. W. Berry, A. M. Childs, R. Cleve, R. Kothari, and R. D. Somma, *Phys. Rev. Lett.* **114**, 090502 (2015).
- [13] G. H. Low and I. L. Chuang, *Phys. Rev. Lett.* **118**, 010501 (2017).
- [14] G. H. Low and N. Wiebe, arXiv:1805.00675.
- [15] A. Kalev and I. Hen, *Quantum* **5**, 426 (2021).
- [16] J. Preskill, *Quantum* **2**, 79 (2018).
- [17] M. C. Tran, Y. Su, D. Carney, and J. M. Taylor, *PRX Quantum* **2**, 010323 (2021).
- [18] B. Şahinoğlu and R. D. Somma, *npj Quantum Inf.* **7**, 119 (2021).
- [19] C. Cirstoiu, Z. Holmes, J. Iosue, L. Cincio, P. J. Coles, and A. Sornborger, *npj Quantum Inf.* **6**, 82 (2020).
- [20] M. Möttönen and J. J. Vartiainen, *Decompositions of General Quantum Gates* (Nova Publishers, New York, 2006).
- [21] D. d’Alessandro, *Introduction to Quantum Control and Dynamics* (CRC Press, Boca Raton, 2007).
- [22] D. D’Alessandro and R. Romano, *J. Phys. A* **45**, 025308 (2012).
- [23] G. Vidal and C. M. Dawson, *Phys. Rev. A* **69**, 010301(R) (2004).
- [24] N. Khaneja and S. J. Glaser, *Chem. Phys.* **267**, 11 (2001).
- [25] D. D’Alessandro and F. Albertini, *J. Phys. A* **40**, 2439 (2007).
- [26] B. Drury and P. Love, *J. Phys. A* **41**, 395305 (2008).
- [27] M. Dağlı, D. D’Alessandro, and J. Smith, *J. Phys. A* **41**, 155302 (2008).
- [28] S. Helgason, *Differential Geometry, Lie Groups, and Symmetric Spaces*, Crm Proceedings and Lecture Notes (American Mathematical Society, Providence, 2001), pp. 247–248, Lemma 6.3 (iii).
- [29] H. N. Sá Earp and J. K. Pachos, *J. Math. Phys. (N.Y.)* **46**, 082108 (2005).
- [30] E. Kökcü and T. Steckmann, [github.com/kemperlab/cartan-quantum-synthesizer](https://github.com/kemperlab/cartan-quantum-synthesizer).
- [31] S. Gu, R. D. Somma, and B. Şahinoğlu, *Quantum* **5**, 577 (2021).
- [32] A. Chapman and S. T. Flammia, *Quantum* **4**, 278 (2020).
- [33] See Supplemental Material at <http://link.aps.org/supplemental/10.1103/PhysRevLett.129.070501> for mathematical exposition, proofs and circuit simplification.
- [34] J. Wei and E. Norman, *Proc. Am. Math. Soc.* **15**, 327 (1964).
- [35] A. F. Izmaylov, M. Díaz-Tinoco, and R. A. Lang, *Phys. Chem. Chem. Phys.* **22**, 12980 (2020).

- [36] J. D. Whitfield, J. Biamonte, and A. Aspuru-Guzik, *Mol. Phys.* **109**, 735 (2011).
- [37] A. Jayashankar, A. M. Babu, H. K. Ng, and P. Mandayam, *Phys. Rev. A* **101**, 042307 (2020).
- [38] P. W. Anderson, *Phys. Rev.* **109**, 1492 (1958).
- [39] V. Bucaj, [arXiv:1608.01379](https://arxiv.org/abs/1608.01379).
- [40] E. Kökcü *et al.*, Figure 4 Data From: Fixed Depth Hamiltonian Simulation via Cartan Decomposition, Dryad, Dataset, [10.5061/dryad.r4xgxd2cd](https://doi.org/10.5061/dryad.r4xgxd2cd).
- [41] E. Kökcü, D. Camps, L. Bassman, J. K. Freericks, W. A. de Jong, R. Van Beeumen, and A. F. Kemper, *Phys. Rev. A* **105**, 032420 (2022).
- [42] D. Camps, E. Kökcü, L. Bassman, W. A. de Jong, A. F. Kemper, and R. Van Beeumen, *SIAM J. Matrix Anal. Appl.* **43** (2022).
- [43] L. Bassman, R. Van Beeumen, E. Younis, E. Smith, C. Iancu, and W. A. de Jong, *Materials Theory* **6**, 13 (2022).
- [44] N. F. Berthussen, T. V. Trevisan, T. Iadecola, and P. P. Orth, *Phys. Rev. Research* **4**, 023097 (2022).
- [45] T. Steckmann, T. Keen, A. F. Kemper, E. F. Dumitrescu, and Y. Wang, [arXiv:2112.05688](https://arxiv.org/abs/2112.05688).
- [46] D. Z. Manrique, I. T. Khan, K. Yamamoto, V. Wichitwechkarn, and D. M. Ramo, [arXiv:2008.08694](https://arxiv.org/abs/2008.08694).
- [47] B. T. Gard, L. Zhu, G. S. Barron, N. J. Mayhall, S. E. Economou, and E. Barnes, *npj Quantum Inf.* **6**, 10 (2020).
- [48] F. Albertini and D. D'Alessandro, *Systems and Control Letters* **151**, 104913 (2021).
- [49] J. Chen, H. Zhou, C. Duan, and X. Peng, *Phys. Rev. A* **95**, 032340 (2017).
- [50] D. D'Alessandro and J. T. Hartwig, *J. Dyn. Control Syst.* **27**, 1 (2021).
- [51] X. Wang, D. Burgarth, and S. Schirmer, *Phys. Rev. A* **94**, 052319 (2016).